

VERE

VERE: Virtual Embodiment and Robotic Re-Embodiment

Integrated Project no. 257695

FP7-ICT-2009-5

WorkPackage WP3: *Intention Recognition*

Deliverable D3.3 **Second BBCI Prototype**

C. Hintermüller (GTEC), K. Blom (UB), M. Slater (UB), Robert Jenke (TUM),
Mohammad Abu-Alqumsan (TUM), Nikolas Martens (TUM), Angelika Peer (TUM),
Pierre Gergondet (CNRS), Abder Kheddar (CNRS) Veronica Orvalho (IT), Christoph
Guger (GTEC)

Release date: 04 Jan. 2013

Status: *Public*

EXECUTIVE SUMMARY

This document describes the brain and body computer interface developed in workpackage WP3. It lists the different improvements and parts added to the second prototype. In extension to the first prototype, the EEG based steady state visual evoked potential (SSVEP) and P300 brain computer interface paradigms have been improved. A new code based paradigm allows to administer SSVEP stimuli which do not depend on the refresh rate of the screen and the new statistics based zero class is able to detect when the user is focusing his intention on the BCI controls and prevent any selection in any other case. Methods have been established for online detection of erroneous selections of actions either by the user or the BBCI system using Error related Potentials generated by the human brain. First tests have shown that the implemented algorithms are able to identify and filter about 85% of the errors.

While high-level intentions decide on what should be executed (transformed into a sequence of actions by WP4), low-level intentions aim at modifying how these actions are executed (quality of actions) by taking into account the actual user mental state. The second prototype uses the different frequency bands of the EEG for a basic discrimination of different emotional and affective states. New facial features have been identified to improve the marker less online facial tracking algorithms implemented in the second prototype. Together it will be used to assess the users affective state and emotions.

Summarizing the BBCI includes now state of the art tracking of body and facial movements and the most sophisticated implementations of motor imagery, P300 and SSVEP based brain-computer interfaces all of them interfaced with the embodiment station. Very important is that for all BCI implementation the accuracy and robustness was highly increased and a zero class detection was implemented.

Deliverable Identification Sheet

IST Project No.	FP7-ICT-2009-5 – Project 257695
Acronym	VERE
Full title	VERE: Virtual Embodiment and Robotic Re-Embodiment
Project URL	http://www.vereproject.eu/
EU Project Officer	Christiane WILZECK

Deliverable	
Work package	WP3 Intention Recognition

Date of delivery	Contractual	M 30	Actual	
Status	version. 1.0		Final <input checked="" type="checkbox"/>	
Nature	Prototype <input checked="" type="checkbox"/> Report <input type="checkbox"/> Dissemination <input type="checkbox"/>			
Dissemination Level	Public <input type="checkbox"/> Consortium <input checked="" type="checkbox"/>			

Authors (Partner)	C. Hintermüller (GTEC), K. Blom (UB), M. Slater (UB), Robert Jenke (TUM), Mohammad Abu-Alqumsan (TUM), Nikolas Martens (TUM), Angelika Peer (TUM), Pierre Gergondet (CNRS), Abder Kheddar (CNRS), Veronica Orvalho (IT), Christoph Guger (GTEC)			
Responsible Author	C. Hintermüller		Email	hintermueller@gtec.at
	Partner	GTEC	Phone	+43 7251 22240 17

Abstract (for dissemination)	The second BBCI prototype was successfully developed and installed at several VERE partner institutions. First studies are already successfully running.
Keywords	BCI, physiological monitoring system, P300, SSVEP, CSP, error potentials, emotions, zero class, facial tracking

Version Log			
Issue Date	Rev No.	Author	Change
23.10.2012	001	C. Hintermüller	First Draft
05.11.2012	002	V. Orvalho	Adding description of facial tracking
13.11.2012	003	A. Peer, R. Jenke, M Abu-Aqumsan	Adding description of ErrP detection, affective state
26.11.2012	004	C. Hintermüller, P. Gergondet	Adding description of CSP, coded based SSVEP, Zero-Class and Considerations for stimulation and trainging
27.11.2012	005	C. Guger	Added description of BCI

30.11.2012	006	C.Hintermüller	Added secription of ECoG mapping system developed, and first test
04.01.2013	1.0	C. Hintermüller	

TABLE OF CONTENTS

EXECUTIVE SUMMARY	II
TABLE OF CONTENTS	V
1 INTRODUCTION	1
2 INTENTIONS	1
2.1 Block Diagram.....	2
I8	3
3 USER INTENTIONS	4
3.1 P300 Paradigm.....	4
3.1.1 Probability based Classification and Selection.....	5
3.1.2 Face Speller	6
3.2 Code based SSVEP Paradigm	8
3.2.1 Zero Class	10
3.3 Motor Imagination BCI	12
3.4 Rapid functional mapping of the cortex using ECoG	13
3.5 System Layout	15
3.6 Remote Stimulus Display	17
3.7 Merging Video stream and SSVEP	18
4 COGNITIVE STATE	19
4.1 Error Potentials	19
4.2 Experimental setup	19
4.3 IErrP Pilot study	20
4.4 Preprocessing	20
4.5 Classification and preliminary results	21
4.5.1 Gaussian classifier	21
4.5.2 Hidden Markov Models (HMM)	21
4.6 Concluding remarks and future work	22
5 AFFECTIVE STATE	22
5.1 Preprocessing: Artifact removal	23
5.2 Feature Extraction and Feature Selection.....	24
5.3 Classification and Results.....	26
5.4 Future Work:	26
5.5 Facial Emotion Tracking	27
6 QUALITY OF EXPERIENCE	28
6.1 Visual Stimulation Improvement.....	28

7 BCI SYSTEM INSTALLATIONS..... 31
8 REFERENCES 32

1 INTRODUCTION

The goal of workpackage 3 is to develop a system for identifying the intentions of the user and to extract their different components and aspects. There exist different levels of intentions. High level intentions include all goal oriented intentional actions and plans such as grabbing a glass or walking to the cinema whereas low level intentions represent all actions and behavior which is not directed towards a specific goal. They typically define how a high level intention, a goal oriented action, is performed, the level of commitment to it, by considering e.g. different emotional states. The Brain and Body Computer Interface System (BBCI) records biosignals like the EEG, ECG, the respiration or the galvanic skin response of the user’s body. It extracts the physiological parameters and features thereof and uses them to generate measures which represent both types of user’s intentions.

The second prototype of the BBCI adds algorithms to detect the so called Error related Potentials (ErrP). These can be used to filter commands or actions selected by the BBCI system which do not correspond to the users intention. The proper commands are passed to the robotic and virtual avatar controller system. The remaining biosignals such as ECG, galvanic skin response, etc. and related physiological parameters like heart rate or respiration rate are recorded and mapped to different qualities of robot actions in WP4.

In the following section 2 the components of the second BBCI prototype and the interfaces between them are shown. The block diagram helps to clarify the description and to visualize all required interactions between the BBCI components.

2 INTENTIONS

Throughout the work in VERE, we differentiate between high- and low-level intentions, by which we mean the intentions that describe *what* and *how* actions and commands are carried out, respectively. Sensory data (EEG and other physiological data) is mapped in the intention recognition module to high- and low-level intentions as can be seen in Figure 1.

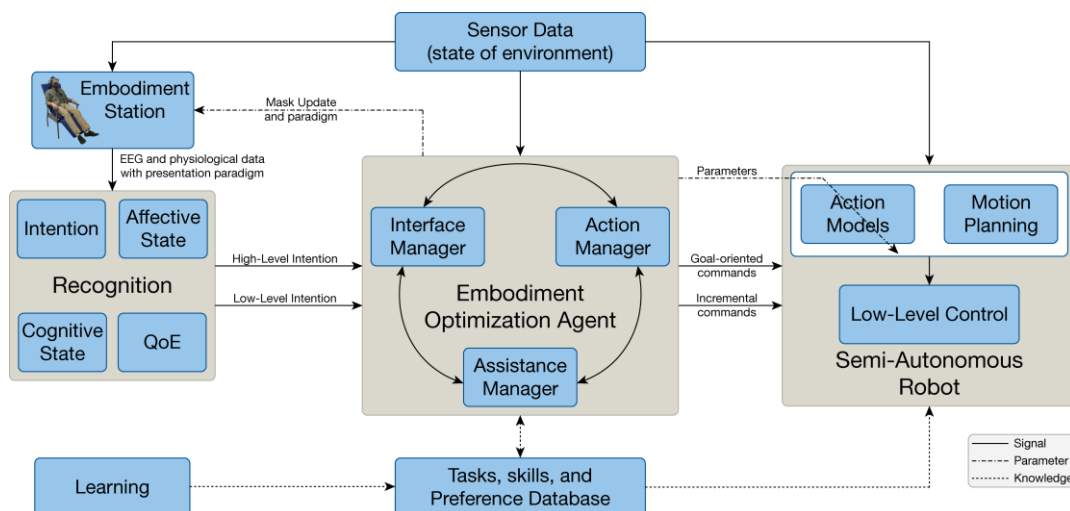


Figure 1: Interconnection of intention recognition module and robotic re-embodiment system

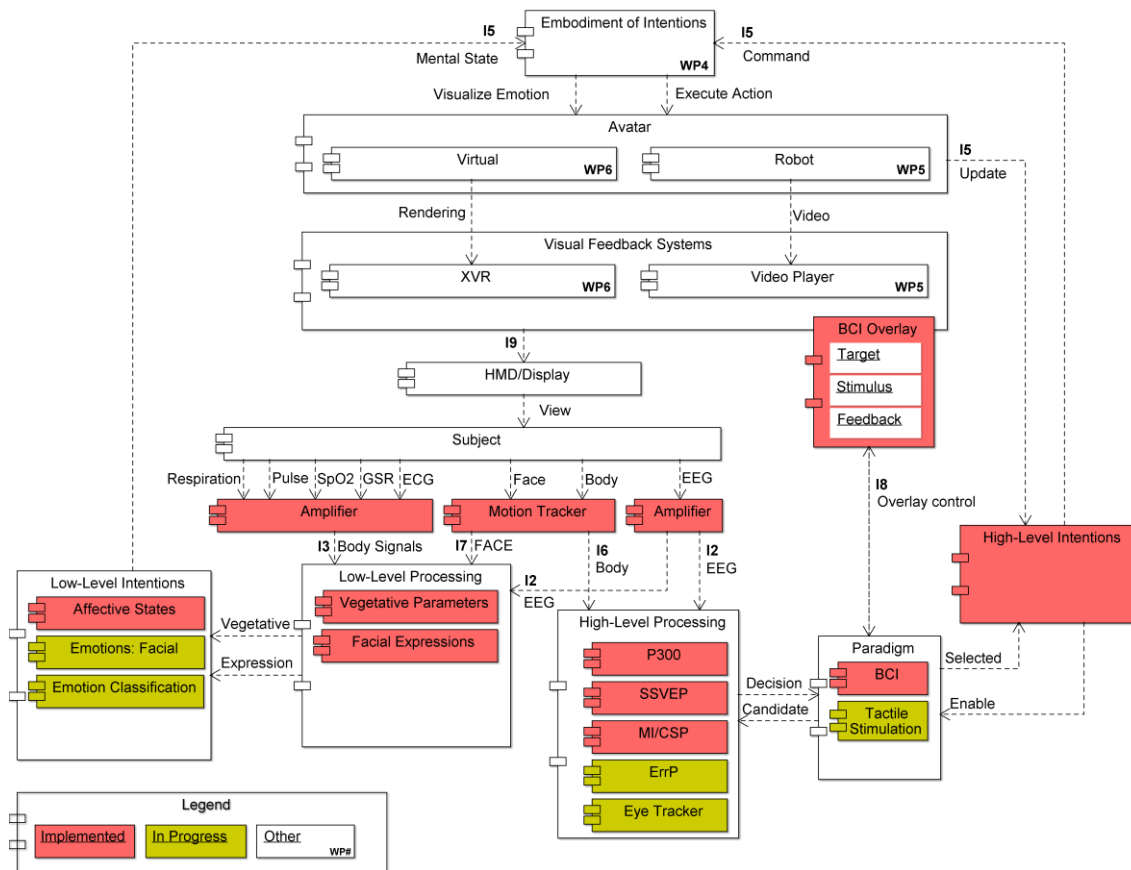
We define *high-level intentions* as what users intend to do or what actions they intend to perform. The recognition module maps the sensory data (from EEG or other physiological sensors) to user high-level intentions. Further, the human cognitive state can be reduced to a yes/no user command as in [1], and hence it can be also interpreted as high-level intention.

We define **low-level intentions** as how an action or command should be carried out. Low-level intentions include emotions (affective state), some cognitive states (user workload, stress, fatigue and error awareness) and the perceived Quality of Experience (QoE). QoE is a subjective metric that reflects user's experience with a provided service. It comprises aspects of using a system or a service, as well as including experience-related aspects of the presented content itself.

2.1 Block Diagram

A block diagram of the main hardware devices and software components of the BCI system is shown in Figure 2. The dashed lines represent the interfaces between them and the arrows indicate the direction along with the data and information are passed onwards to the next component. The arrow labels indicate the data to be exchanged between the different components. The interfaces **I2, I3, I5, I6, I7, I8** and **I9** interconnect the BCI prototype system with the components of the VERE prototype developed within other workpackages. These interfaces have been defined and described in detail in deliverable D3.1.

Basically, two types of intentions are recognized by the BCI system, i.e. high-level and low-level intentions. The high-level commands recognized via the active BCI paradigm (e.g P300 or SSVEP) are passed on to the next system blocks for the embodiment of the intentions on the robot (WP4,5) or the virtual avatar (WP4,6). Herein, it is decided how these commands are interpreted and it is decided how they are executed on the virtual or robotic avatar in succeeding work packages. The low-level intentions are processed in parallel to the high-level intentions. While high-level intentions are mapped in WP4 into a sequence of robot actions, the low-level intentions determine the quality of how these single actions are implemented.



- I1 fMRI interface; not included in the second prototype and thus not shown
- I2 Active EEG electrodes and biosignal amplifier including g.USBamp driver and MATLAB/Simulink API
- I3 Biosignal sensors for ECG, respiration, galvanic skin response, SpO₂, pulse and biosignal amplifier including g.USBamp driver API
- I4 Knowledgebase interface for High- and Low-Level intention processing (not shown)
- I5 XML interface between multimodal intention recognition system and avatars
- I6 Body motion recording interface
- I7 Facial motion recording interface
- I8 BCI overlay control interface
- I9 binocular image display interface of the head mounted displays

Figure 2: Block diagram of the first BCCI prototype including the connections and interfaces to components developed within the workpackages 2, 4, 5 and 6.

3 USER INTENTIONS

Different BCI paradigms will be used to record the high-level intentions of the user. The second BCI prototype implements a motor imagination (MI) paradigm (section 3.3) in addition to the stimulus based P300 (section 3.1) and SSVEP (section 3.2) paradigms. Compared to the latter two paradigms which recognize a target stimulus the user is attending to, a MI based BCI detects the intended movement or the imagination thereof generated by the user, for example, the left hand. The BCI translates mental signals auto generated by the user or evoked by a target stimulus to predefined xml strings which closely correlate to the high-level intentions the user most likely has within a specific situation.

One of the biggest problems of BCI systems is to detect the zero class, meaning to detect if the person is not intending to make a selection. BCI systems perform with very high accuracies if different states are classified against each other, but the accuracy drops down if the resting state is considered. But to switch off a BCI system and not making any decision it is crucial to be also able to detect the resting state. Therefore in the Y2P an important step forward was made by adding the zero class to all BCI principles: P300, motor imagery and SSVEP.

Methods have been developed to detect Error-related Potentials (ErrPs) and progress has been made to recognize user's cognitive error states. It is possible to identify interaction ErrPs which indicate user awareness of errors related to a false target chosen by the interface or an erroneous selected target symbol. First efforts have been done to extend the recognition of ErrPs to BCI paradigms, like P300 and SSVEP, to obtain an instantaneous verification and validation of the identified intention. Ignoring user interactions, which are followed by ErrPs, leads to higher information transfer rates [2-4].

3.1 P300 Paradigm

Whenever an unlikely event which is awaited by the user occurs randomly between other events a so called P300 evoked potential is elicited. It manifests itself in a positive deflection in the amplitude of the EEG signal around 300 ms after a visual stimulus onset.

For a P300 spelling device commonly a 6x6 matrix of different characters and symbols is presented on a computer screen [5]. In single-character mode all characters are flashed in a random order but only one character after each other as shown in Figure 3a. In row-column mode a whole row or a whole column flashes at a time as shown in Figure 3b. The subject has to concentrate on a specific letter he or she wants to write. The flashing of exactly this character or the corresponding row or column is a relative unlikely event which induces a P300 component in the EEG signal reaching its maximum amplitude around 300 ms after the onset of the flash. For all other characters, rows or columns no such P300 component is elicited because they are not relevant to the subject currently. The accuracy of the P300 spelling devices is increased by presenting the stimuli several times to the user. The results of all individual repetitions are collected and the symbol which elicited the most P300 components is finally selected.

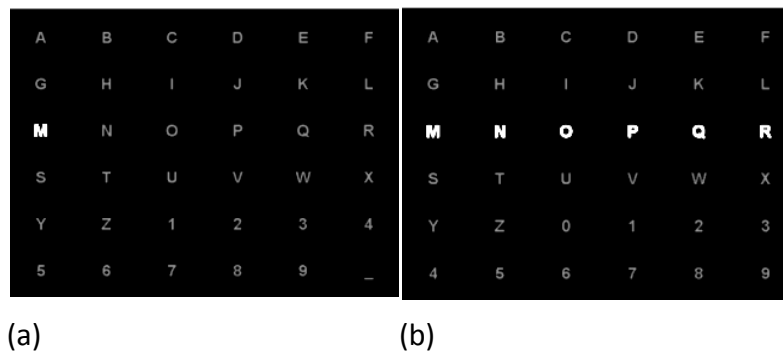


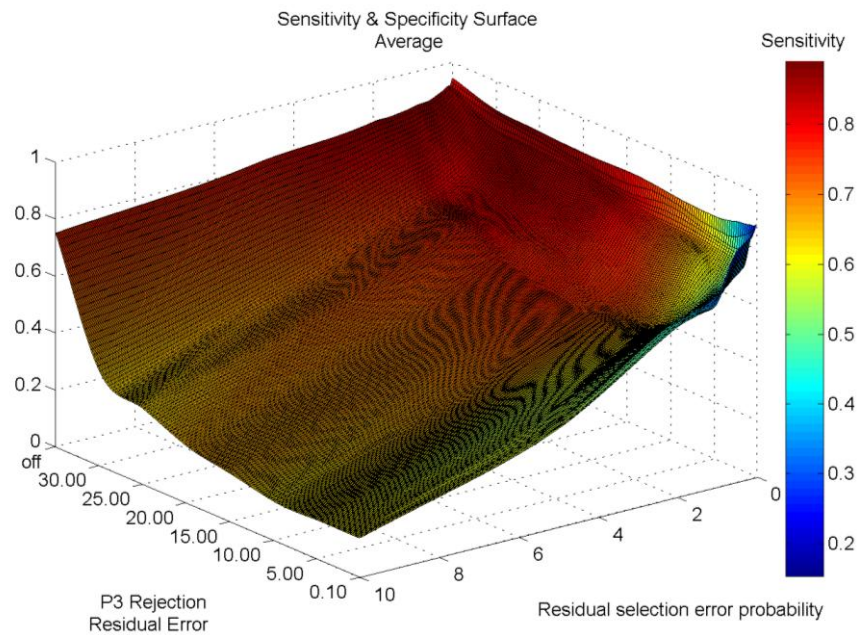
Figure 3: Screen layout of a 36 character speller. Either a single character is highlighted (a) at a certain time or a whole row or column (b).

3.1.1 Probability based Classification and Selection

The detection of the P300 signals was further improved by computing the probability that the user has generated a P300 response for a specific stimulus. The probabilities are computed based on the discriminant scores computed for each stimulus using the so called SoftMax transformation. After every repetition the corresponding probabilities are estimated based on the global sum of all feature scores collected so far. In case the probability exceeds a pre defined limit the flashing will stop immediately and the identified symbol will be displayed to the user. In case no symbol can be found for which the global probability exceeds the limit, no symbol is selected.

In addition to this global probability, the probabilities for each individual trial can be analyzed to assess whether the user is distracted or not paying attention at all to the BCI stimuli. If no P300 component can be found for any stimulus the data of the corresponding repetition is discarded and the user may repeat it.

The limits used for detecting when the user is not paying attention and whether he has selected anything are defined through the maximum acceptable probability that a wrong decision is made by the P300 processing system. Both residual error probability values have an impact on how accurately the chosen action matches the users intention and how responsive and sensitive the system is. Figure 4 shows the achievable accuracy and sensitivity achieved for different error probability values used to do the selection and to reject repetitions the user was not attending to the stimuli. Further the number of required repetitions is listed for a global residual error probability dependent on the limit used to reject individual repetitions.



Parameters considered		Average			# Repetitions								
		SN [1]	SP [1]	FAR [1]	TTP			FTP			FP		
					min	mean	max	min	mean	max	min	mean	max
P3 selection error probability [%]	off	0,85	0,92	0,05	2,22	6,71	13,89	3,00	4,75	7,00	3,33	6,58	9,67
	30,0	0,86	0,84	0,11	2,22	7,50	18,00	11,20	12,77	15,60	3,75	10,03	16,38
	25,0	0,86	0,82	0,12	2,22	7,84	17,67	12,75	15,31	18,25	3,75	9,95	16,25
	20,0	0,84	0,81	0,14	2,22	8,38	18,56	4,00	9,28	13,00	3,50	9,94	17,25
	15,0	0,82	0,79	0,16	2,33	8,72	19,33	8,00	9,89	11,57	3,38	11,18	20,00
	10,0	0,74	0,77	0,17	2,33	9,55	22,33	4,57	7,88	11,57	2,63	13,60	25,00
	5,0	0,64	0,75	0,20	3,78	10,91	22,22	10,29	12,40	14,86	5,78	16,10	22,56
	2,5	0,53	0,74	0,26	2,88	11,83	23,88	14,43	16,64	19,00	7,00	16,70	22,78
	1,0	0,35	0,73	0,33	3,75	13,07	23,63	12,75	15,40	18,25	9,33	19,47	25,00
	0,5	0,26	0,84	0,40	5,75	13,29	20,75	13,38	15,40	17,63	12,56	20,93	25,00
0,1	0,13	0,84	0,51	10,57	14,88	20,57	20,00	22,60	25,00	14,22	22,39	25,00	

Figure 4: The specificity (height) and sensitivity (shading) of the P300 processing system depend on the residual error probabilities used to reject individual repetition runs and to do the final selection after several repetitions. The table lists in addition the minimum, maximum and average number of required repetitions, for properly selected symbols (TTP), improper selected symbols (FTP) and symbols selected when the user was not paying attention at all (FP)

3.1.2 Face Speller

In the second year g.tec evaluated new stimulation methods for the P300 speller. Ten subjects between 23 and 58 years participated in the tests. All of them had to complete 4 different spelling tasks. In the first they had to spell the word Lucas using the classical black and white speller, which uses colour inversion to generate the different stimuli (Figure 5a, c).

In the three other tasks the symbols were replaced by greyscale and colour images of Albert Einstein (Figure 5d, e) and various other celebrities such as Chuck Norris when flashed (Figure 5b, f).

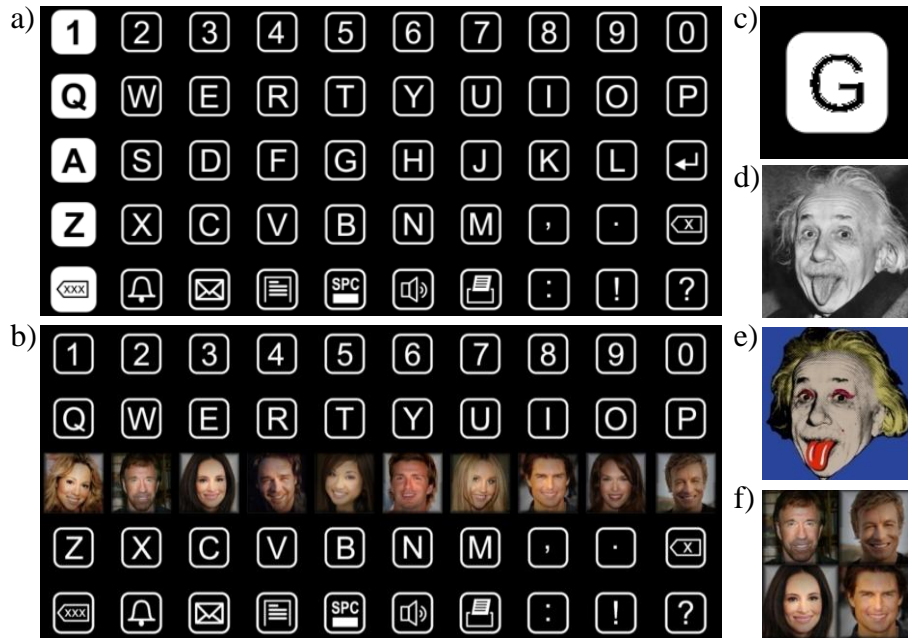


Figure 5: P300 speller masks for comparing the classical speller (a) with different variants of the face speller (b). In total the user had to spell the selected word Lucas in inversion mode (c) and using a gray scale (d) and “pop-art” (e) version of the face of Albert Einstein to highlight the characters. In a final run colour images of several different celebrities were displayed (f) instead.

Guger et al showed that the P300 speller gives a grand average accuracy of around 91 % with 81 subjects in 2007. With the new face speller implementation the group reached 100 % accuracy (Figure 6). This is a very important step forward to increase the robustness of the P300 speller and is worldwide the most sophisticated implementation. The study is currently prepared for publication. We could also show that the P300 speller gives high accuracies with dry electrodes [6]. This is important for a faster montage and a higher acceptance of the BCI system.

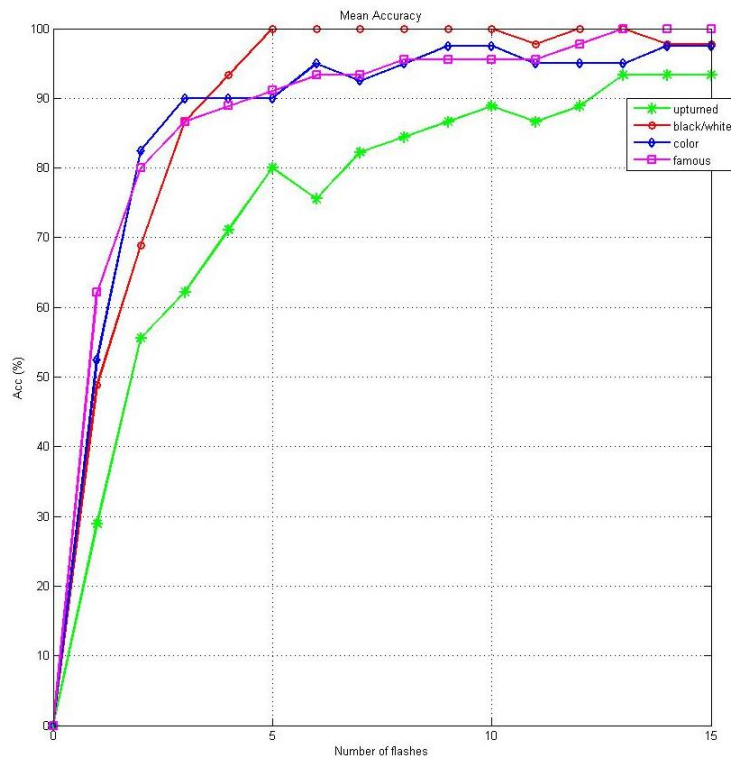


Figure 6: Accuracy achieved by the subjects using the classical P300 speller and the faces speller. For any type of the face speller the users were able to spell without making any mistake with only 5 repetitions compared to the classical speller.

3.2 Code based SSVEP Paradigm

The steady state visually evoked potential (SSVEP) is elicited, if a subject is exposed to a visual stimulus which is repeated with a frequency of at least 6 Hz. For example, a flickering LED can be used as stimulating device. In the second year prototype a code based SSVEP (c-VEP) paradigm was implemented in addition to the frequency coded SSVEP available from the first year prototype. The c-VEP utilizes a random sequence of phases where the LED or the on screen stimulus is switched on or off. The sequence is selected such that new dissimilar random sequences can be generated by adding a phase shift.

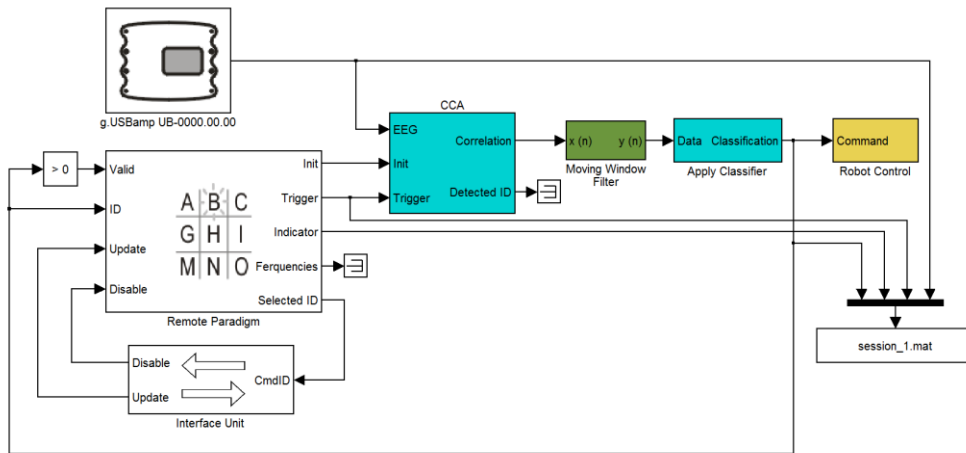


Figure 7: Simulink model of the c-VEP based BCI with on-screen stimulation. The CCA block evaluates the phase information every 200 ms.

These phase shifts are reflected within the EEG spectra observed when the user is attending to c-VEP stimuli. The canonical correlation analysis is used to match the EEG data against a template generated during the training phase (Figure 7). The resulting correlation signals are smoothed and classified with respect to the BCI control selected by the user. The advantage of using c-VEPs for onscreen stimulation compared to frequency coding is that c-VEP’s do not strictly depend on the refresh rate of the computer screen, the Head Mounted Displays (HMD) or the 3D projection system. Table 1 compares two f-VEP setups (LED and onscreen stimulation) with the new onscreen c-VEP stimulation and the plot in Figure 8 shows the average accuracy achieved by 11 subjects over time.

Table 1: Mean and maximum accuracy values achieved by 11 subjects when using LED and onscreen based f-VEP and c-VEP stimulation patterns to control an SSVEP BCI. The buffer length was selected to be 2 seconds for all experiments.

Subject	f-VEP LED Accuracy [%]		f-VEP onscreen Accuracy [%]		c-VEP onscreen Accuracy [%]	
	mean	max	mean	max	mean	max
1	98.65	100.00	98.14	100.00	<u>98.29</u>	100.00
2	75.72	90.00	77.14	95.00	<u>90.39</u>	95.00
3	88.44	95.00	83.05	90.00	<u>95.85</u>	100.00
4	85.57	95.00	97.26	100.00	<u>93.42</u>	95.00
5	100.00	100.00	100.00	100.00	<u>95.83</u>	100.00
6	96.63	100.00	95.09	100.00	<u>97.97</u>	100.00
7	40.76	55.00	42.48	50.00	<u>80.49</u>	95.00
8	72.45	80.00	80.77	85.00	<u>95.00</u>	100.00
9	84.62	90.00	89.28	100.00	<u>96.88</u>	100.00
10	77.19	90.00	62.75	80.00	<u>96.84</u>	100.00
11	100.00	100.00	100.00	100.00	<u>98.66</u>	100.00
mean	83.64	90.45	84.18	90.91	<u>94.51</u>	98.64
std-dev	16.58	12.69	17.25	14.59	<u>4.98</u>	2.23

Each curve represents the average accuracy of eleven subjects and 20 trials. The accuracy values were calculated every 200 ms. The data was smoothed using a moving median window filter with a window size of 1 second for c-VEP and 2 seconds for f-VEP. Nevertheless, the c-VEP configuration reaches a higher accuracy level in shorter time, compared to the f-VEP based BCIs. With the c-VEP setup the eleven users were able to control the BCI with an average classification accuracy of up to 98.64% compared to 90.45% and 90.91% for the two f-VEP setups. This is a very good result for the grand average accuracy.

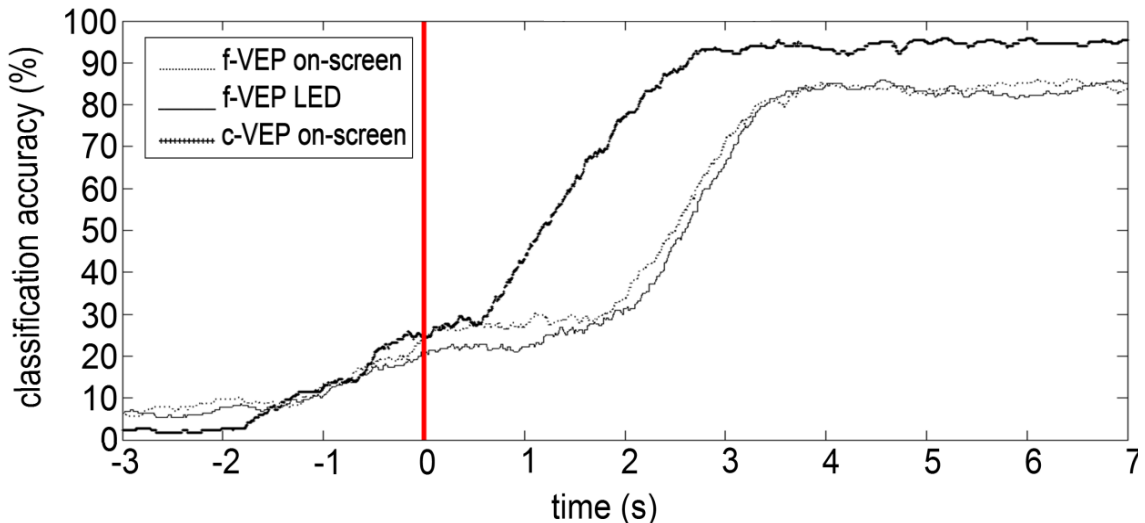


Figure 8: Online accuracy test for the three configurations: c-VEP on-screen, f-VEP on-screen, f-VEP LED. The vertical bar indicates the start of visual stimulation. The EEG buffer was 2.1 s for the c-VEP system and 2 s for the f-VEP systems. A moving median filter of 1 s for c-VEP and 2 s for f-VEP was used to smooth the data.

3.2.1 Zero Class

A pseudo zero class was implemented to provide an idle state, which is used, when the user has no target selected or is not attending at all. This is achieved by rejecting any classification result, for which the residual error probability is larger than a predefined limit. Thereby a SoftMax function is used to transform the output of the discrimination function into the corresponding probability value.

A standard SSVEP feedback experiment was conducted to assess the classification accuracies which were achieved by 11 individual subjects after 20 trials in total. Table 2 compares the accuracies achieved for different types of SSVEP stimuli. Figure 9 shows that the zero class reduces the rate of false positive selections to values close to zero.

Table 2: Classification accuracy with pseudo zero class over 20 trials in total. The performance of all three configurations was evaluated: f-VEP LED, f-VEP on-screen and c-VEP on-screen.

Subject	f-VEP LED	f-VEP on-screen	c-VEP on-screen
#	mean accuracy (2.0 s buffer) (%)	mean accuracy (2.0 s buffer) (%)	mean accuracy (2.1 s buffer) (%)
1	97.63	93.46	88.63
2	8.28	34.24	64.45
3	57.02	38.33	83.24
4	31.93	77.88	86.32
5	90.48	86.73	80.98
6	90.12	81.41	91.21
7	0.00	0.68	20.47
8	39.71	8.43	65.64
9	53.18	47.75	92.64
10	40.19	18.96	53.50
11	100.00	100.00	91.34
mean	55.32	53.44	74.40
std-dev	33.76	34.23	21.08

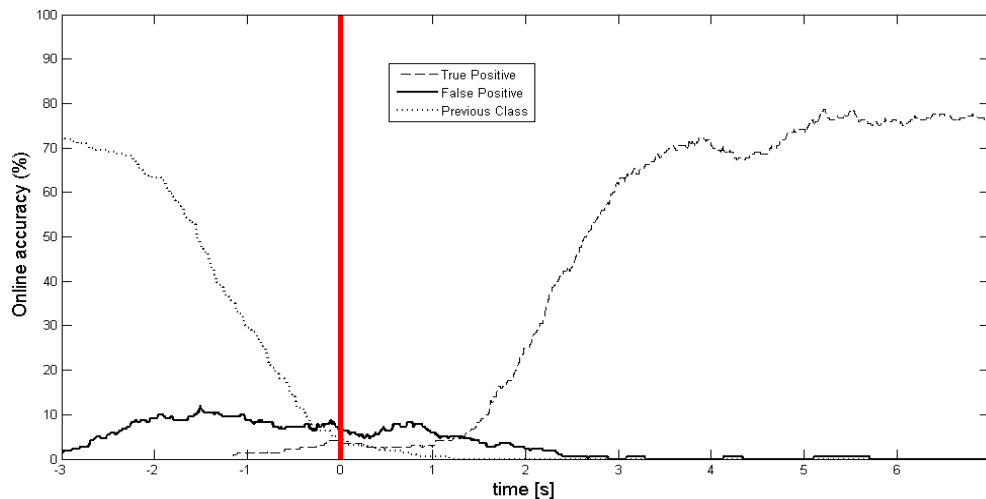


Figure 9: The zero class clearly reduces the number of false positive selections.

The zero class implementation allows now to avoid decision when the user is not intending to make one, but of course this reduces also the classification accuracy. With a window size of 2 seconds a good compromise was made between an acceptable false positive rate and a fast decision time. For some application more robustness is more important and this can be realized with a longer time window, if the BCI system should be faster a shorter window can be used. It is also possible to tune this window length in real-time in future for optimizing the decision speed.

Summarizing the current SSVEP implementation is also state of the art and was recently published in [7] because of its high grand average accuracy not achieved before.

3.3 Motor Imagination BCI

Whenever the subject executes a movement or at least imagines the movement, this is reflected within the EEG signals recorded from the motor cortex. In VERE the common spatial pattern (CSP) method is used to extract and analyze the related features. The CSP based system, shown in Figure 10, is able to discriminate a movement of the left hand from a right hand movement. Utilizing the zero class as described in section Zero Class, it is in addition possible to detect whether the user has generated a movement at all.

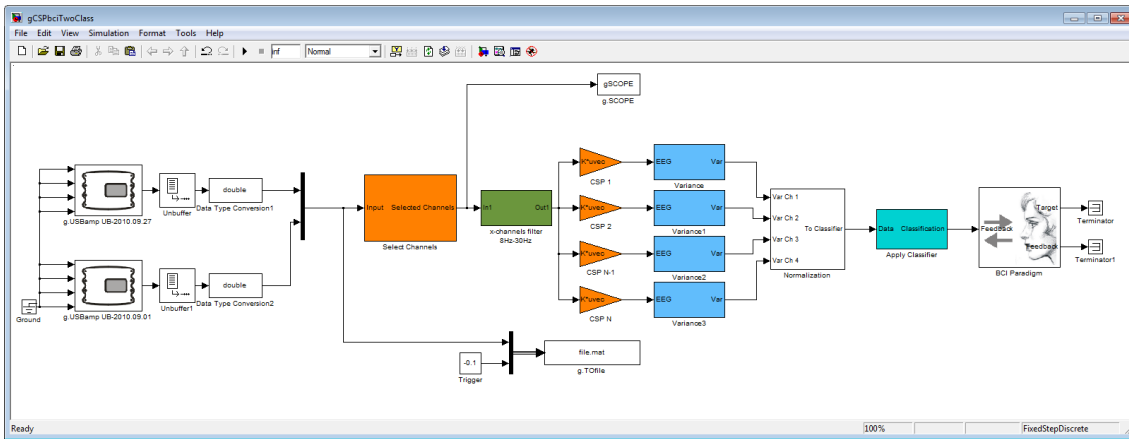


Figure 10: Motor Imagination BCI using common spatial patterns to identify the users intention and motor commands.

The number of channels used for CSP varies between 16 and 64 channels. The setup shown in Figure 10, uses two g.UBSamp amplifiers with 16 channels each. Therefore the maximum channel number is 32. To be able to record from both devices the amplifiers have to be connected with the synchronization cable. During the training phase for example a horizontal bar can be used to provide the user with a cue which movement he should generate (Figure 11).

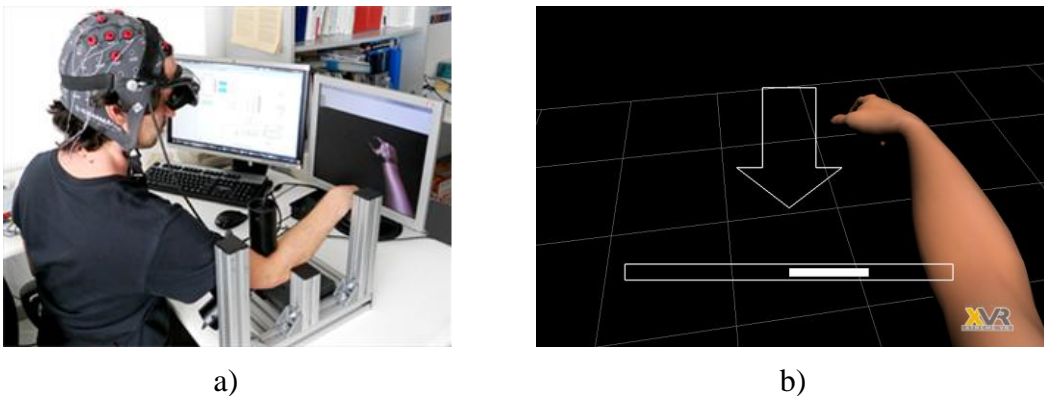


Figure 11: Different feedback modalities used in connection with the CSP based BCI. a) Proprioceptive stimulation generating the illusion that the arm is moving. b) Feedback generated by the movement for the virtual arm and the horizontal bar.

Studies with healthy subjects showed that the increase of electrode channels increases also the communication speed and accuracy. With the 64 channel CSP setup a grand

average accuracy of 80 % could be achieved. This is much higher than with any other motor imagery implementation existing and is currently prepared for publication. In the study it could also be shown that 19 out of 20 subjects could control a MI based BCI system after a short training interval of about 90 minutes. Before this study it was generally accepted that MI based BCI system don't work for the majority of people.

3.4 Rapid functional mapping of the cortex using ECoG

The BCI systems described above measure the brain's electrical activity from the surface of the scalp noninvasively. They rely on the EEG whereas ECoG based systems have numerous advantages over EEG systems, including (i) higher spatial resolution, (ii) higher frequency range, (iii) fewer artifacts, and (iv) no need to prepare users for each session of BCI use, which usually requires scraping the skin and applying electrode gel. Recent research has demonstrated, over and over, that ECoG can outperform comparable EEG methods because of these advantages.

g.tec has developed the CortiQ software for ECoG based rapid functional mapping of the cortex. It is used to identify functional brain regions in real-time with invasive sensors. Using that data, the system constructs and continuously updates a Mental Activity Profile (MAP). This MAP is unique for each patient, reflecting which brain areas are active during specific functions. Medical experts can get more relevant information than previously possible, presented in a straightforward fashion with clear and helpful images, with less work than currently required. CortiQ takes advantage of existing ECoG grids and consists of the following additional components (see Figure 12):

1. Biosignal amplifier – high quality biosignal amplifier with 24 Bit and 256 channels
2. Real-time processing system – high performance real-time control unit to manage all devices in real-time, to analyze the signals and to visualize and store data
3. Mapping system – high performance source localization and mapping system based on SIGFRIED mapping technology



Figure 12 The system components of the ECoG system.

The software allows doctors to position the electrode grids they used (which can be selected from a library) over a schematic brain map. Patients perform different mental tasks. In the first experiments a Ritaccio-Paradigm was used. It includes five different tasks (i) solving Rubik's-Cube, (ii) shaking the neck (iii) stick out the tongue, (iv) kissing and (v) listening to a story. Each of the tasks was split into a resting and an execution phase of 15 seconds duration each. Thereby it could be verified that the ECoG system was able to evaluate and display the activation difference in the high gamma frequency range, between the resting and the active state for all electrodes simultaneously in real-time.

The high gamma activity is indicated by red circles over relevant electrodes. A large red circle shows that the corresponding electrode is placed over a brain area which is highly involved in that task (see Figure 12-14).

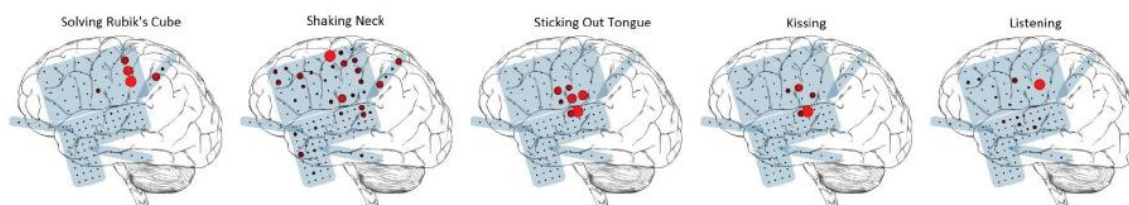


Figure 13: Five different tasks, and the brain areas active during each of them.

Electrical cortical stimulation (ECS) is used to verify the correct electrodes that reflect brain activity during a specific task or action. Multiple grids and strips are often used to cover large cortical areas and results of the ECS are shown in Figure 14, indicating the important brain functions identified.

A patient with 120 subdural electrodes, which were implanted for clinical resection procedure, participated in a first test. Figure 13 shows the results obtained for γ -Mapping using the Ritaccio-paradigm. The acoustic areas as well as the motor areas controlling the movement of hand, lips and tongue correlate very well with the ECS

results shown in Figure 14. The advantage of the high-gamma based mapping is that it allows to generate maps of active brain regions within minutes and is less affected by epileptic seizures or pain observed by the patient.

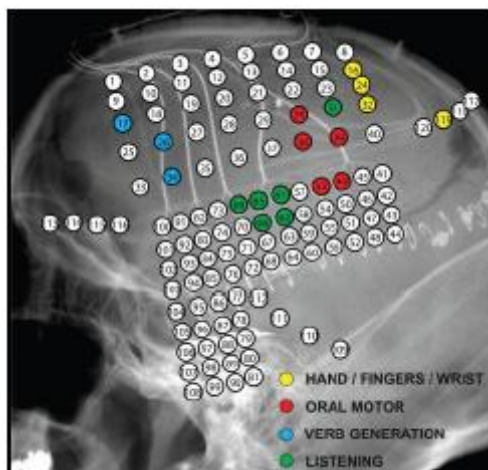


Figure 14: Electrical cortical stimulation (ECS) results for hand/finger/wrist movement, oral motor, verb generation and listening (image courtesy of Gerwin Schalk, Wadsworth Center, USA).

3.5 System Layout

All types of BCI systems are embedded within the rapid prototyping environment (RPE) described in deliverable D3.1. Figure 15a shows the basic structure of the P300 system. The EEG data is recorded through the biosignal amplifier from g.tec, bandpass filtered and down sampled to 64Hz. The signal processing block evaluates the P300 responses and computes the ID of the selected symbol. The paradigm block displays the control mask (Figure 15b) and drives the flashing of each single symbol in single character mode and each row and column in RC mode in random order. After each character or row and column has flashed the configured times, indicated by the stop signal of the Processing block the Paradigm block sends the ID of the selected control to the Interface Unit block. The later sends the command string configured along with the displayed symbol to the intention embodiment system of the VERE prototype (Deliverable D4.1) for interpretation and execution.

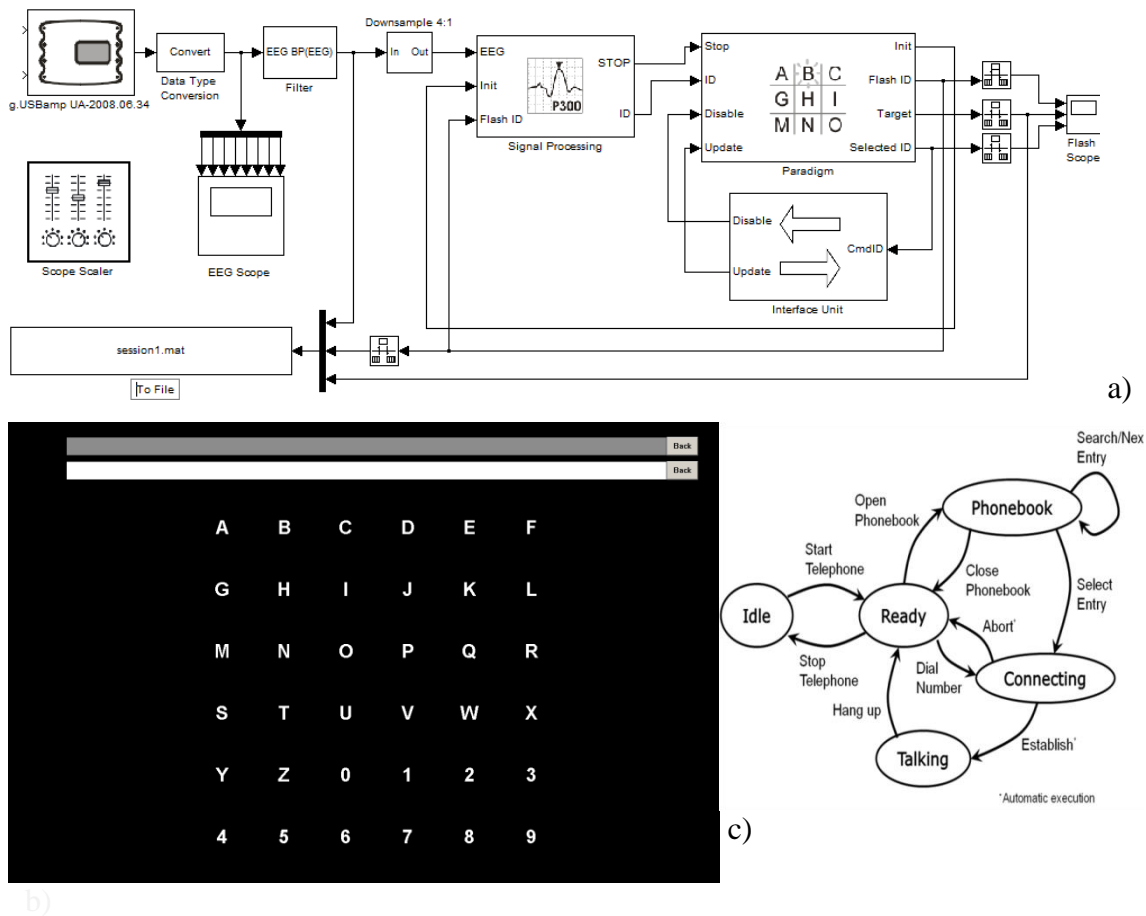


Figure 15: a) Brain Computer interface system implemented in Matlab/Simulink. It is based on the P300 paradigm. The Interface Unit block implements the interface I5 which interconnects the BCI unit of the high level intention recognition systems with the components developed within the other workpackages (WP4, WP5 and WP6) b) Spelling mask for writing texts or chatting. c) State diagram for defining the commands available when using for example a phone through the BCI.

The whole system can be adapted to the intended application through an XML formatted configuration file. This file contains the size of the control mask, the address of the components developed by the other workpackages (WP4, WP5 and WP6) which shall receive the command strings associated with each single symbol. The system even allows defining multiple levels of masks. It is advisable to generate for each target system a so called state diagram as shown in Figure 15c. It describes the states of the client system which shall be accessible through the BCI system and all possible transitions between these states and their direction. The arrows representing these transitions are labelled with the names of the commands which shall initiate the transition. If necessary these labels may include additional parameter values, in case one single command is able to trigger multiple related transitions. Details on how to configure the BCI system are available from the user manual distributed along with the system and from g.tec.

The structure of the SSVEP based system is shown in Figure 16. Four visual stimuli at frequencies of 7.5Hz, 8.5Hz, 10Hz and 12Hz are generated by the BCI Overlay module

described in the following section 3.6. During the training mode a green frame indicates to the user at which SSVEP stimulus he has to focus on. The ID number of each SSVEP element directly corresponds to the command which shall be executed by any of the attached components of the VERE prototype. As for the P300-based system the Paradigm block interrelates these IDs with the intended action which is transmitted via the Interface Unit block to the attached component of the VERE prototype.

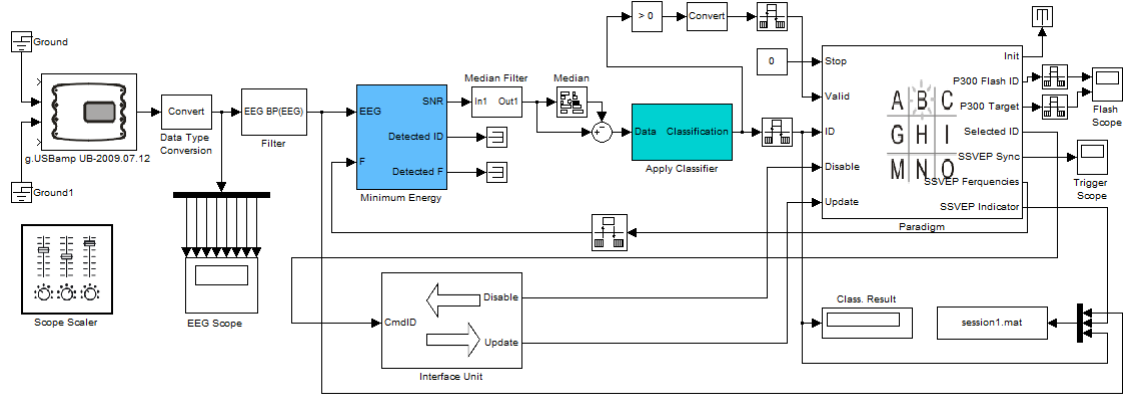


Figure 16: BCI based on the steady stated visual evoked potential paradigm.

3.6 Remote Stimulus Display

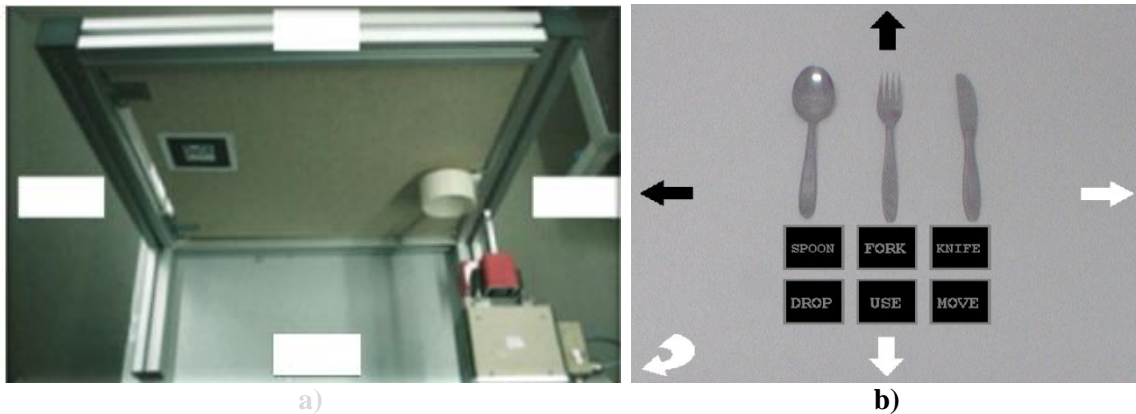


Figure 17: BCI controls displayed on top of a life video streams. a) User observes a robot opening a door and controls it via simple SSVEP controls. b) User is presented SSVEP controls for steering the camera and P300 controls for utilizing a knife, a fork and a spoon.

As users need to get the visual feedback of the environment from the perspective of the robot or their physical avatar, a stereo camera (two 2D cameras) is mounted on the robot and keeps transmitting the captured frames to users. With the help of Head-Mounted Displays, users are able to have the full 3D experience of the robot environment. The visual feedback system is developed within the workpackages WP2, WP5 and WP6.

Through the interface **I8** it is possible to merge the stimuli required by the BCI system with the video stream from the cameras of the robot or the virtual scenery created by the modules developed in WP5 and WP6. The combination of video stream and BCI

controls enables the user to observe the environment, the set of possible actions and the effects of their executed actions. Figure 17 shows examples of what users might see when wearing the HMD. In Figure 17a the SSVEP paradigm is overlaid on the video stream received from a robot while opening a door. The example in Figure 17b shows the combined display of SSVEP and P300 controls. In both examples the display for only one eye (left or right) is shown.

The BCI controls are generated by the BCIOverlay module DLL which the visual feedback system loads and initializes when needed during runtime. This DLL uses native OpenGL commands to draw the P300 and SSVEP stimuli and the different symbols and characters representing the different actions the user may execute through the attached avatar.

The module is controlled by and connected to the BCI paradigm block (Figure 15a and Figure 16a) through a bidirectional network socket connection using the UDP network protocol. Whenever a set of stimuli P300 or SSVEP are presented to the user the module indicates this by sending a trigger message indicating the highlighted controls to the BCI Paradigm block over the UDP socket. These trigger signals are then converted and distributed to the Simulink blocks for the P300 and SSVEP processing.

This is an important step forward to allow the same user interface for the video feedback and BCI controls and solved also a technically very demanding issue of being able to stimulate at constant frequencies or with stable codes on a video stream. It is currently the only BCI system supporting this mode. The work is currently submitted to a journal.

3.7 Merging Video stream and SSVEP

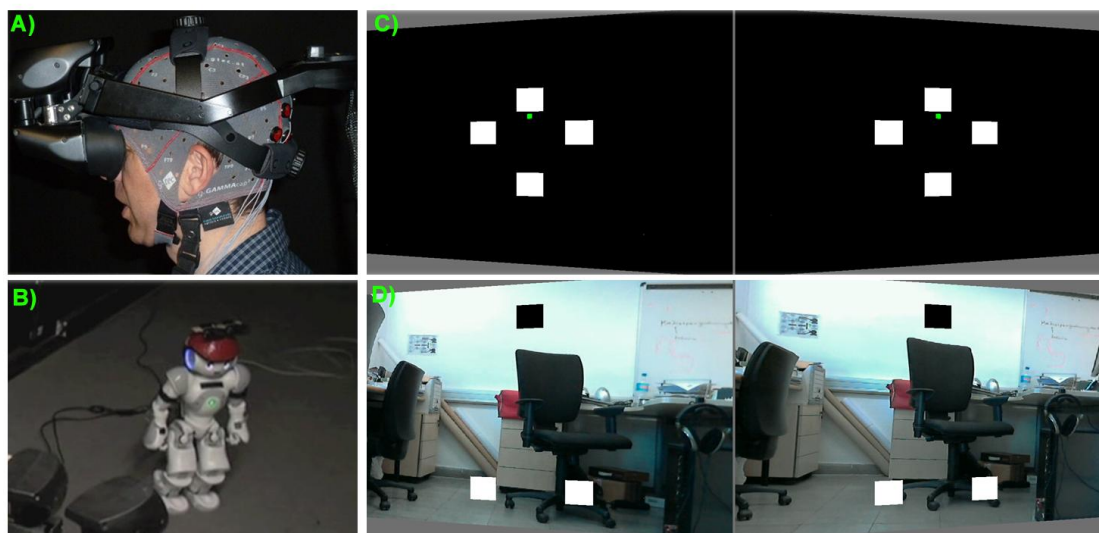


Figure 18: Fig. A) The participant wears the Head Mounted Display on top of the EEG cap. B) The robot has two cameras mounted at averaged eye distances to generate an stereoscopic vision for the participant. D) For the participant the view was as if he was inside the robot. C) The SSVEP stimulation boxes seen by the participant during the training session.

The main aim of this experiment was to test if SSVEP stimulation could work normally inside HMDs (Figure 18A). The major concern was whether different ways in which stimulation was applied separately to both eyes (Figure 18C) would generate the same kind of activation in the visual cortex as a regular SSVEP showed on a computer screen does (Figure 18D). Besides, once we found out that separate stimulation for each eye worked with high levels of accuracy, we tested an application in which you are able to control a robot as if you were inside of it.

A newer version of this experimental proof of concept was recently covered by the Euronews Sci-Tech Futuris program, under the title "A world without limits". This work has been done as in Universitat de Barcelona with a close collaboration with gTec.

4 COGNITIVE STATE

We use the term cognitive state to indicate user workload, stress, fatigue and error awareness.

4.1 Error Potentials

Interaction Error-related potentials (ErrPs) are special features that can be detected in the EEG, after a wrong action selection by the BCI system or the user. After the onset of the feedback indicating the selected action, these features can be distinguished by first, a sharp negative peak after 250 ms followed by a positive peak after 320 ms and a second broader negative peak after 450 ms [3].

4.2 Experimental setup

In a first experiment similar to the one described in [3], we tried to explore interaction ErrPs in the case of erroneous keyboard interactions. Thereby the user was asked to push a ball into a hole which is located on the same horizontal line as the ball using keyboard left and right arrow keys only. The user input was translated by the interface into movements of the ball, thereby it moved the ball into the wrong direction with a probability of error P as shown in Figure 19. The recognition of the ErrPs is challenging due to the low signal-to-noise ratio (SNR) inherent in single trials, as opposed to averaging number of trials in case of P300. The combined usage of the interaction ErrP paradigm with SSVEP and P300 is part of our future work.

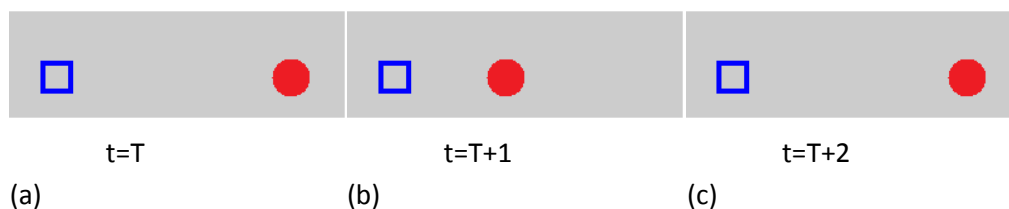


Figure 19: Experimental setup for interaction ErrPs. Using left and right arrow keys, the user should bring the ball (red circle) into the hole (blue rectangle). As an example, the initial positions of the ball and the hole, are shown in (a). The user hits the left arrow button to move the ball closer to the hole, and the result is shown in (b). Interaction ErrPs are evoked when the user hits the left arrow button and the ball goes to the right as shown in (c). Erroneous interactions reduce the information transfer rate ITR, e.g. $ITR=0$ for this example.

4.3 IErrP Pilot study

One healthy male subject (25years) has participated in the pilot study. We used g.tec's gUSBamp to acquire the EEG data with 256Hz. Based on the extended 10-20 system, 32 active electrodes were placed at positions FP1, FP2, F7, F8, F3, F4, T7, T8, C3, C4, P7, P8, P3, P4, O1, O2, AF3, AF4, FC5, FC6, FC1, FC2, CP5, CP6, CP1, CP2, Fz, FCz, Cz, CPz, Pz and Oz. One passive ground electrode was placed at FPz. Signals were referenced to the right earlobe.

The distance between the ball and the hole was 2 steps. The user played the game in 5 sessions, on the same day. Each session consisted of 20 game trials.

Overall we collected 74 erroneous trials (with the label ErrP) and 264 correct trials (with the label noErrP). In this case, the probability of error P was set to 20%.

4.4 Preprocessing

In order to reduce noise in the acquired EEG signals, the average potential over the 32 channels at each time sample was subtracted from each channel. Channels were then filtered with a 1-10 Hz bandpass filter, and down-sampled to 64Hz.

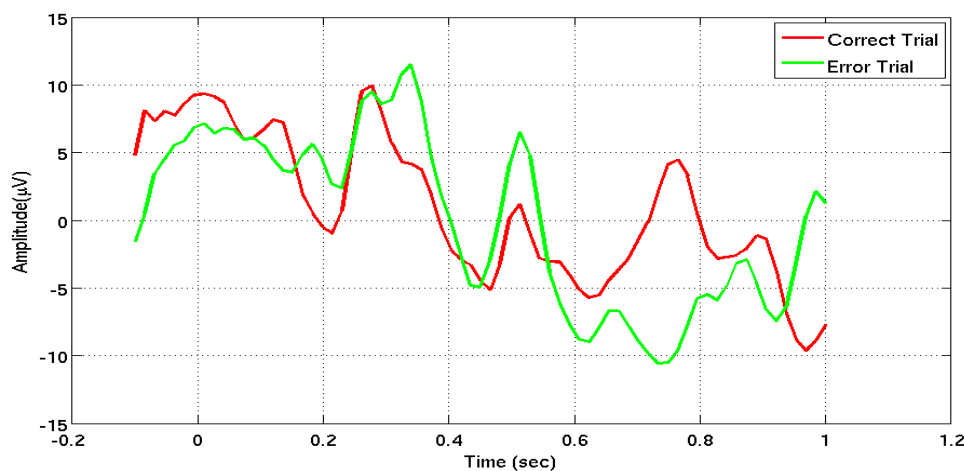


Figure 20: Correct and Erroneous trials (after preprocessing) at Cz electrode

As can be seen in Figure 20, single trials do not show distinguishable features, due to their low signal-to-noise ratio. The trial averaging for electrode Cz is shown in Figure 21.

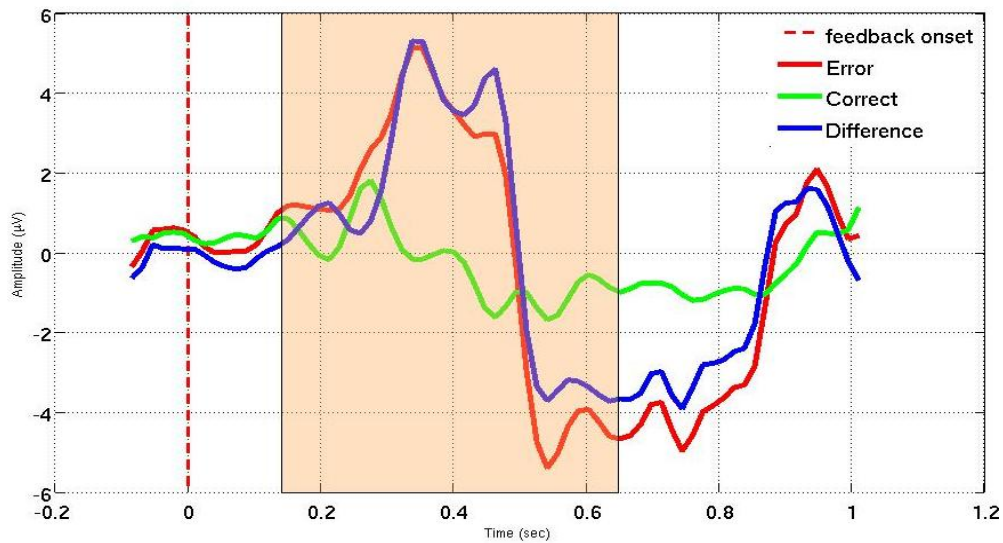


Figure 21: Trial averaging at Cz for erroneous and correct trials

For classification, time samples within the interval [0.15s, 0.65s] after the onset of the feedback are considered as in [3].

4.5 Classification and preliminary results

4.5.1 Gaussian classifier

The Gaussian classifier reported in [2, 3] is considered as state-of-the-art baseline. A superposition of N Gaussians is assumed to constitute the class-conditional probability density function. These Gaussians are first initialized with self-organizing map algorithm and then updated iteratively to minimize the mean square classification error. This optimization is achieved with a stochastic gradient descent algorithm.

Our implementation of the Gaussian classifier is identical to [2], except that we use k-means clustering to initialize the Gaussians. Results for 10-fold cross-validation are shown in Table 3

Table 3: Classification results for the Gaussian classifier

Label	Accuracy
ErrP	0.95 ± 0.05
noErrP	0.72 ± 0.12

4.5.2 Hidden Markov Models (HMM)

As HMMs allow to capture the temporal structure of signals, we have also implemented an HMM classifier with 4 hidden states and 1 Gaussian per state. Results for 10-fold cross-validation are shown in Table 4.

Table 4: classification results for the HMM classifier

Label	Accuracy
ErrP	0.72 \pm 0.09
noErrP	0.64 \pm 0.05

4.6 Concluding remarks and future work

The results of the pilot study shows that the Gaussian classifier [2, 3] still gives the best classification results. As the number of parameters that need to be estimated during the HMM training is relatively high, in future experiments we will record more labelled EEG data.

The simulated-BCI experiment discussed in this deliverable will be compared to P300- and SSVEP-based BCIs. We aim at examining the presence of IErrPs after wrong interactions resulted from misclassification of selective-attention BCIs.

Additionally, we plan to perform experiments with different subjects to examine the inter-subject variability and to analyze whether different users need completely different classifiers.

5 AFFECTIVE STATE

The database presented in D3.2 has been further studied and the framework for emotion recognition from EEG and physiological signals has been built. First results are presented within this document.

The recorded dataset consists of 16 subjects, each containing 8 trials of 30s EEG recording for each of the 5 different emotions (happy, curious, angry, sad, quiet). The emotions were induced using IAPS pictures [8].

Since induction is generally assumed to take about 10s for an emotion to be induced and an emotion lasts for about 4s, time intervals between 11 s-15 s of the recording are tested in the following. In agreement with this finding, we found separability of single features to increase in this segment.

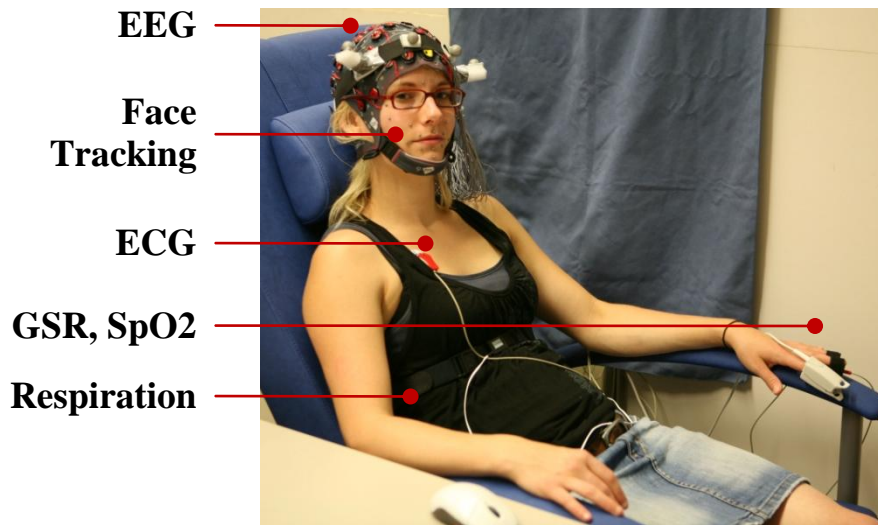


Figure 22: Sensors of emotional database.

A major challenge in emotion recognition from EEG signals relates to interpersonal variance in both emotion induction and recognition. It is not in general agreed upon, which features are most appropriate for this task. Different people have different emotional responses and thus, different features of the EEG data carry the best information for recognition. Additionally, the vast amount of possible features makes it necessary to reduce dimensions in order to avoid under-sampling and over-specification. The work presented in the following introduces the framework implemented for emotion recognition, i.e. database summary, artifact removal, feature extraction, feature selection, and classification (see Figure 23). Further, we investigate differences in classification success rates between features selected on an individual basis versus selection on inter-individual basis.



Figure 23: Systematic overview of the emotion recognition framework.

5.1 Preprocessing: Artifact removal

ICA based plug-in ADJUST for the MATLAB Toolbox EEGLAB is used to identify and remove different kind of artifacts: eye-blinks, eye-movements, drift, and generic discontinuities.

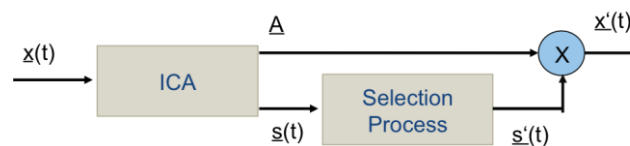


Figure 24: ICA signal flow graph used for artifact removal.

The algorithm first transforms EEG data into Independent Components (ICs) as depicted in Figure 24. In the selection process, artifact-affected components are detected and discarded automatically by ADJUST. Finally, the inverse transformation of the remaining components is computed. An example of this processing step is shown in Figure 25

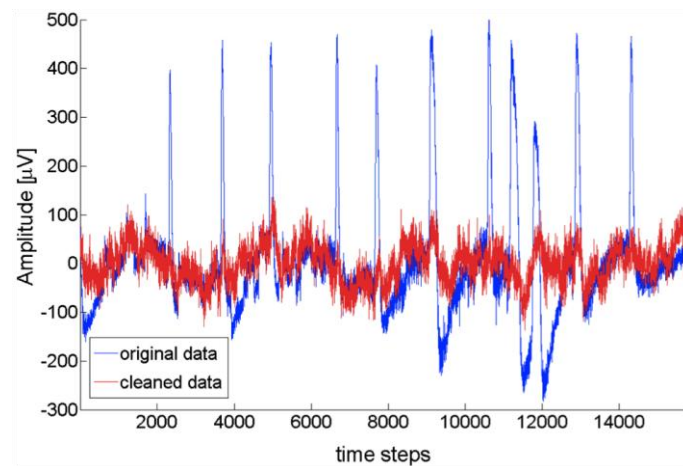


Figure 25: Example of artifact removal.

5.2 Feature Extraction and Feature Selection

We implemented a variety of features found in literature and applied a univariate feature selection filter method to find important features. A list of features from both the time and frequency domain is given below:

Frequency domain:

- Theta-band (4-8Hz)
- Alpha-band (8-12Hz)
- Beta-band (14-30Hz)
- Gamma-band (43-68Hz)

Time domain:

- Power of Signal
- Hjorth Feature [9]:
 - o Activity
 - o Mobility
 - o Complexity

For each of the frequency domain features, we use *mean*, *max*, *min*, and *var* of the computed FFT values. Features are *z*-normalized to zero mean and standard deviation equal to one.

For Feature selection, we compute the statistical effect size f^2 of each feature as a measure of separability. Features are chosen in decreasing order of effect size. Figure 26a shows the mean (color) and variance (radius of black circle) of the effect size values averaged over all subjects mapped to the electrode positions on the scalp.

Although for most features the important (i.e. high f^2) areas overlap, some of those have high variance. In some cases, this even means a feature is only suitable for one subject (see Figure 26b below), but does not separate classes well for other subjects. Meanwhile, features scoring high f^2 values and low variance are considered generally suitable across subjects. We compare feature selection based on an individual's effect size of a feature and on average effect size of each feature over all subjects with each other.

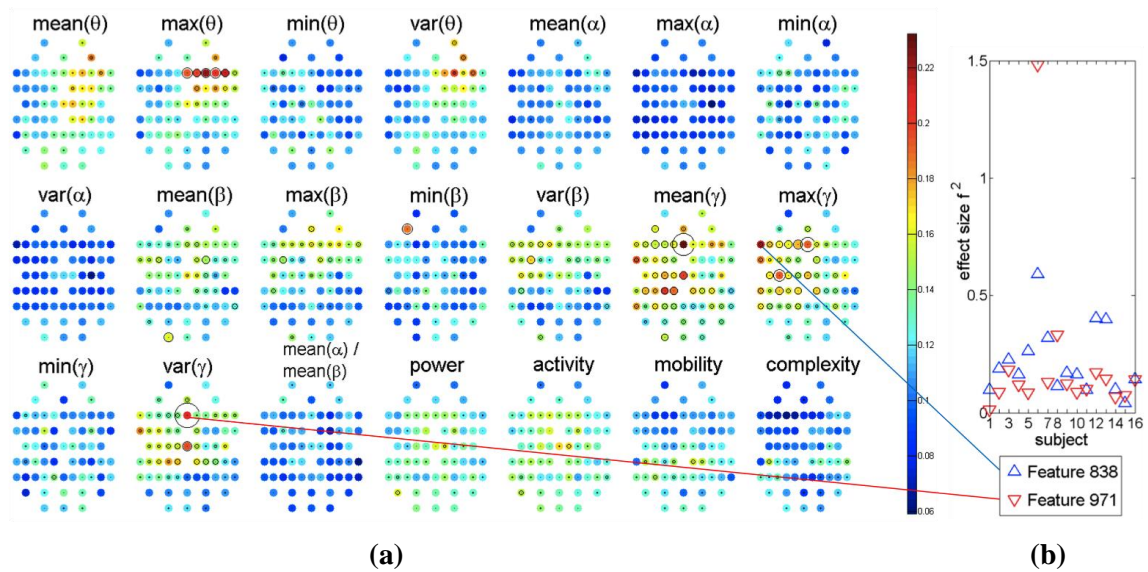


Figure 26: (a) Mean (colorbar) and variance (radius of black circle) of f^2 over all subjects, each plot corresponds to one feature, (b) Example of two features individually.

5.3 Classification and Results

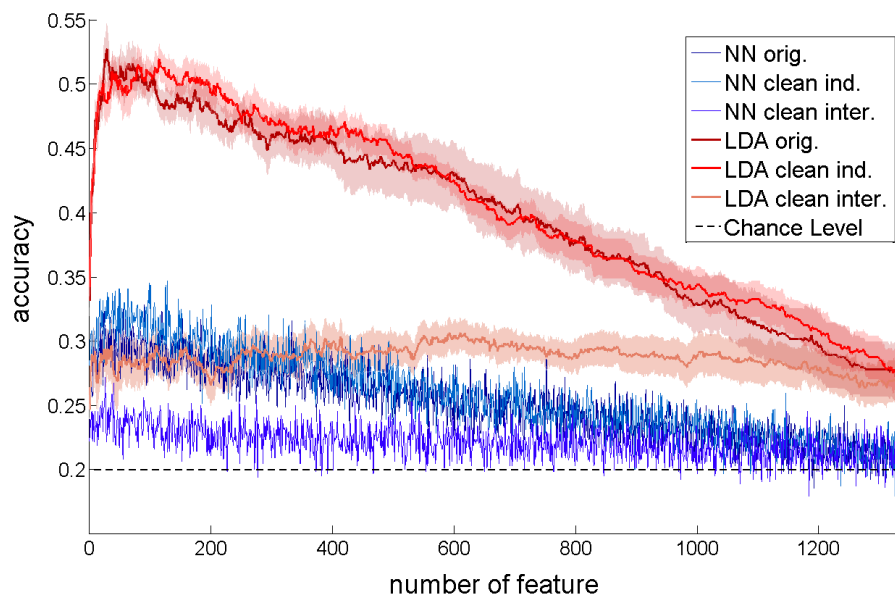


Figure 27: Classification results for LDA (red, including inter-subject variance) and Neural Networks (blue) for different artefact removal and feature selection.

Classification is done by means of LDA and Neural Network (1 hidden layer, 20 neurons). We use leave-one-out cross-validation to evaluate the proposed feature selection methods. Classifiers are trained and tested for each newly added feature.

Individual feature selection results in a significantly higher average success rate than feature selection based on averages over all subjects.

The applied artifact removal does increase average classification rates of the Neural Network classifier, but shows little effect for LDA (the maximum accuracy is even slightly decreases).

Generally, the ‘curse of dimensionality’ is clearly visible, as accuracy steadily decreases for an increasing number of features. Feature selection is thus crucial for successful classification of emotional EEG data. Comparing to traditionally used regions of the brain, our results suggest that sometimes features different from literature separate well, especially on an individual basis.

5.4 Future Work:

In the future, we want to extend classification to continuous emotional dimension using the PAD Model [10], e.g. by using Neural Networks. We intend to further improve feature selection based on methods taking into account dependence between features.

Additionally, the results gained from EEG signals should be fused with other modalities. These are, for example, physiological features like heart rate, skin resistance or the respiration rate. The g.tec software to extract those signals (as introduced in D3.2)

will be used in addition to other prevalent features found in literature. We are currently working on an implementation of this.

5.5 Facial Emotion Tracking

Development of facial recognition systems had stimulated the research of facial features inherent to the expression of emotions. In this section, it was aimed to know which features truly influence face configuration during the expression of certain emotion and built a modular system of emotion detection (happy, sad, angry, disgusted, surprise, fear and contemptuous), which will be crossed with BCI system.

The first method developed for emotion classification was an off-line approach based in image filtering and segmentation. Since the last method is based in image filtering, lightning changes and non-static poses strongly affects the accuracy of emotion detection. To overcome these problems a new method was developed. This method is based in a constrained facial features extraction, where a restricted number of facial features tracked is selected and compared to the neutral pose (Figure 28). Using a Randomized random forests machine learning method, this system can track the six basic Ekman's emotions in real time with an accuracy of 88 %. However, a manual calibration with neutral face has to be done to each person.

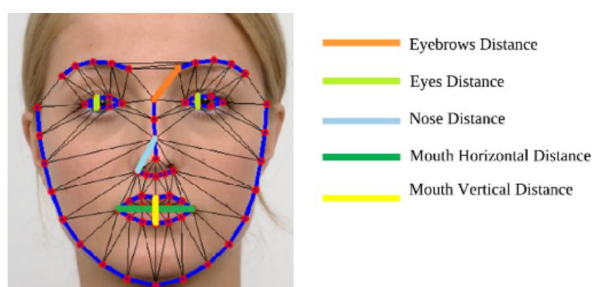


Figure 28 – Constrained facial features in emotion classification: Measured distances between selected landmarks generated by the face recognition system (red points). These distances are calculated in real time in relation to the neutral expression.

To produce an automatic method, another study was done and new geometrical features were defined. Thus, using the same facial recognition prototype of the last method, 19 landmarks are extracted and used to calculate two classes of features: eccentricity and linear (Figure 29). These features are used to train a random forests machine learning method and allow the real time emotion prediction. Compared to state of the art emotion classification methods available, this method allows real time and automatic emotion classification of the six basic Ekman's emotions without calibration or manual intervention, not compromising the accuracy of detection (89%). This work is currently submitted to the conference Eurographics 2013.

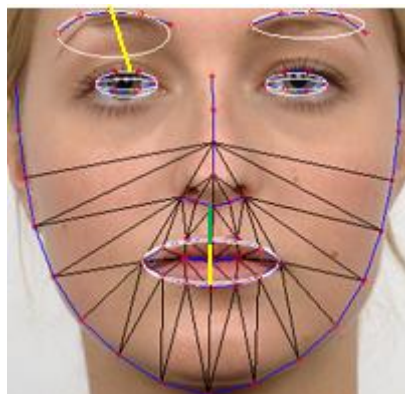


Figure 29 – Geometrical features extracted for emotion classification: eccentricity features (white ellipses) and linear features (green and yellow lines).

The emotional database used where the Radboud database [9]. This multicultural and multi poses database is characterized by contain 67 real person's face models performing 7 pure emotions (contemptuous plus six basic Ekman emotions).

Through the affective state experiment described before, a performance study using the last geometrical emotion classifier will be done. In case of success, an experiment plan including BCI emotion detection will be created. On the other hand, in case of failure, a novel method will be developed. Possible causes for failure may be due to the not enough detection accuracy of the method, since emotions expressed during the experiment tend to be subtle and our method was trained using a pure expressions database. Therefore, the new emotion classifier will have the following features:

- Real-time and fully automatic emotion classification;
- Sensitivity to subtle facial features;
- Partial Occlusions and face asymmetries may be supported;
- Vectorial information to describe direction of facial features motion;
- Weighted result to the six Ekman's basic emotions per frame.

Then, the new method will be submitted to stressing tests, firstly detecting only emotions using facial features and, secondly, crossing data from EEG systems.

The major challenges of this method will be to retrieve a weighted result from the machine learning algorithm without compromising the accuracy and the impact of the visual paradigm on facial emotions expressions.

6 QUALITY OF EXPERIENCE

6.1 Visual Stimulation Improvement

The color [11, 12], frequency [13] and shape of the stimulus greatly impacts the quality of the SSVEP and thereby also the quality of the BCI experience. In [14], an extensive review of SSVEP-related works is presented. It shows that three kinds of stimuli are currently used in SSVEP experiments: physical LED, on-screen flickering shape and on-screen checkerboard stimuli. On-screen stimuli are commonly used within applications with a rich feedback such as virtual reality navigation [7]. However, the

stimuli are displayed on top of this feed-back which might hide important elements from this feedback and also make the experience less immersive for the user.

The SSVEP has been used extensively in robotic control application within the VERE project. We proposed to use techniques from computer vision to extract objects of interest within the field of view of the robot and display an SSVEP stimulus on top of this object to indicate to the user a possible interaction.

The goal of this research is to compare different flickering methods to obtain similar detection, and thus control accuracy while having less obtrusive stimuli. The different methods that are being tested are shown in Figure 31 to 36.

During the experiment, we record the activity of the brain; we use the same electrodes' position as in SSVEP detection, see Figure 30. The user successively looks at different flickering objects with different frequencies- ranging from 6 Hz to 12 Hz - and different flickering conditions.

During a recording session, the user looks at a flickering object for 10 seconds. After a 5 seconds break he concentrates on the next object. The parameters of all selection elements such as the frequency are known to the experimenter. Once all flickering elements have been attended by the user for one object he switches his focus to another object. This cycle is repeated 3 times for each object.

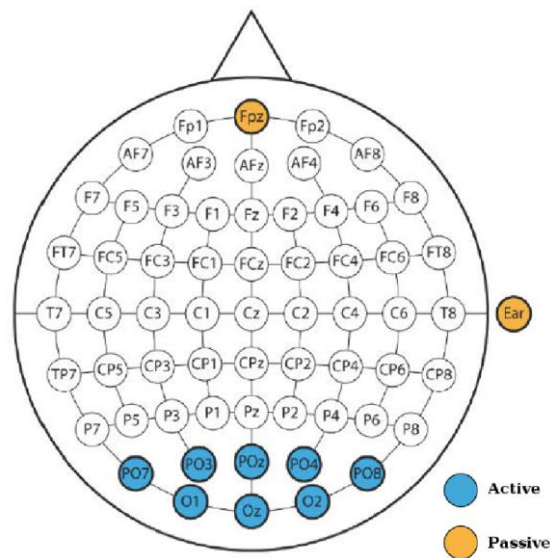
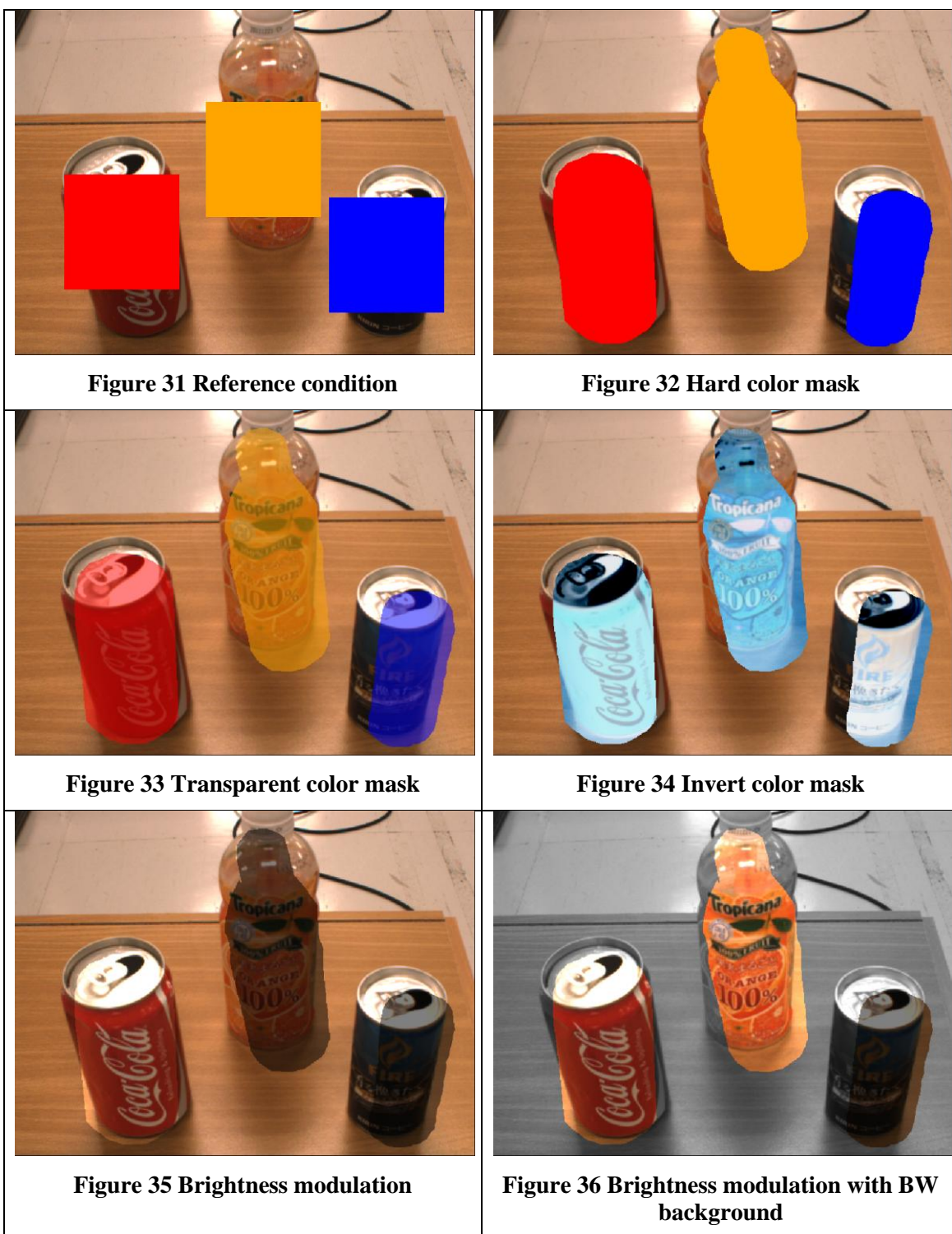


Figure 30 Electrodes positions for signal recording



After the recording session, the user is asked to rank the flickering methods according to his/her preference.

On the other hand, we look at the power spectrum of the recorded signals to determine which flickering method triggers the strongest answer. Segments of 3 seconds duration were used to compute the spectrum. For each trial of 10 seconds length the spectrum was recomputed every 200 milliseconds. Figure 37 illustrates the mean power

of the signals in laplacian derivation $L2 = 4 \times OZ - O1 - O2 - P07 - P08$ for a trial subject.

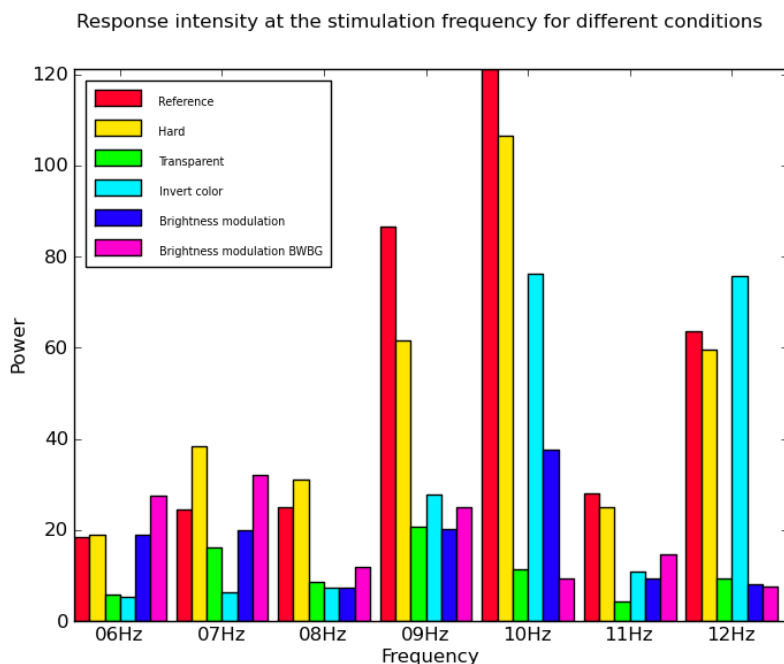


Figure 37 Power measurement at stimulation frequency (trial result)

Using statistical analysis tool we can then determine which stimulation method performs the best at a given frequency. E.g. in the case of L2 at a 7Hz stimulation, we can conclude – for this user – that: Hard > Brightness modulation BWBG > Reference > Brightness modulation > Transparent > Invert color (with $p < 0.01$).

The next step of this research is to conduct test on a larger number of subjects to draw tangible conclusion.

7 BCI SYSTEM INSTALLATIONS

Currently the following partners have running BCI systems

IDC – 16 channel BCI system: SSVEP, P300

EPFL – 48 channel BCI system: CSP

UCL – 16 channel BCI system: CSP

FSL – 16 channel BCI system: SSVEP, P300, CSP

TUM – 32 channel BCI system: SSVEP, P300, EEG, BCIOverlay

CNRS – 16 channel BCI system: SSVEP, P300, BCIOverlay

g.tec – 16 channel BCI system: SSVEP, P300, CSP, BCIOverlay

UB – 8 channel BCI system: SSVEP

IDIBAPS – 16 channel BCI system: SSVEP, P300

PERCO – 16 channel BCI system: SSVEP, P300, CSP, BCIOverlay

8 REFERENCES

1. E. W. Sellers, D. J. Krusienski, D. J. McFarland, T. M. Vaughan, and J. R. Wolpaw, "A P300 event-related potential brain-computer interface (BCI): The effects of matrix size and inter stimulus interval on performance," *Biological Psychology*, vol. 73, no. 3, pp. 242-252, October 2006.
2. P. W. Ferrez and J. d. R. Millán, "You are wrong! - Automatic detection of interaction errors from brain waves," In *Proceedings of the 19th International Joint Conference on Artificial Intelligence*, Edinburgh, UK, August 2005.
3. P. W. Ferrez and J. d. R. Millán, "Error-related EEG potentials generated during simulated brain-computer interaction," In *IEEE Trans. Biomed. Eng.* 55, 923-929, 2008.
4. Schalk, G., Wolpaw, J. R., McFarland, D. J., and Pfurtscheller, G., "EEG-based communication: presence of an error potential". *Clinical neurophysiology*: official journal of the International Federation of Clinical Neurophysiology, 111(12), 2138-44, 2000.
5. E. Donchin, K. M. Spencer, and R. Wijesinghe, "The mental prosthesis: assessing the speed of a P300-based brain-computer interface," *IEEE Trans. Rehabil. Eng.*, vol. 8, no. 2, pp. 174-179, June 2000.
6. Guger C, Krausz G, Allison BZ and Edlinger G Comparison of dry and gel based electrodes for P300 brain-computer interfaces. *Front. Neurosci.* 6:60, 2012
7. Guger C, Allison BZ, Großwindhager B, Prückl R, Hintermüller C, Kapeller C, Bruckner M, Krausz G, Edlinger G. How Many People Could Use an SSVEP BCI?, *Front Neurosci*:169. . 2012,
8. Lang, P.J., Bradley, M.M., & Cuthbert, B.N. (2008). *International affective picture system (IAPS): Affective ratings of pictures and instruction manual*. Technical Report A-8. University of Florida, Gainesville, FL.
9. Hjorth, B. (1970). "EEG analysis based on time domain properties". *Electroencephalography and Clinical Neurophysiology*, vol. 29, 306-310, 1970.
10. J. Russell and A. Mehrabian, "Evidence for a three-factor theory of emotions," *Journal of research in Personality*, vol. 11, pp. 273-294, 1977.
11. D. Regan. "An effect of stimulus colour on average steady-state potentials evoked in man." *Nature*, 210:1056-1057, 1966.
12. Christoph S. Herrmann. "Human EEG responses to 1100 Hz flicker: resonance phenomena in visual cortex and their potential correlation to cognitive phenomena". *Experimental Brain Research*, 137(3-4):346-353, 2001.
13. Danhua Zhu, Jordi Bieger, Gary Garcia Molina, and Ronald M. Aarts. "A Survey of Stimulation Methods Used in SSVEP-Based BCIs". *Computational Intelligence and Neuroscience*, 2010:12, 2010.
14. Josef Faller, Robert Leeb, Gert Pfurtscheller, and Reinhold Scherer. "Avatar navigation in virtual and augmented reality environments using an SSVEP BCI". In *1st International Conference on Applied Bionics and Biomechanics ICABB-2010*, 2010.
15. Brunner P, Ritaccio AL, Lynch TM, Emrich JF, Wilson JA, Williams JC, Aarnoutse EJ, Ramsey NF, Leuthardt EC, Bischof H, Schalk G. (2009). A practical procedure for real-time functional mapping of eloquent cortex using electrocorticographic signals in humans. *Epilepsy Behav.*, 15(3):278-86.
16. Schalk G, Leuthardt EC, Brunner P, Ojemann JG, Gerhardt LA, Wolpaw JR. (2008). Real-time detection of event-related brain activity. *NeuroImage*, 43: 245-249.